SUSPECTED PLUME IMPINGEMENT INFLUENCE ON BOARD CALIBRATION SYSTEM OF TERRA/ASTER/VNIR INVESTIGATED THROUGH TREND ANALYSIS ON BOARD CALIBRATION DATA

K.Arai [a*] , N. Ohgi [b] and H. Inada [c]

[a] Dept. of Information Science, Saga University, 1 Honjo 840-8502 Japan, arai@is.saga-u.ac.jp
[b] Japan Resources Observation System and Space Utilization Organization, 2-24-2 Nichibei Bldg, Hacchobori, Chuo-ku, Tokyo, 104-0032 Japan, nohgi@jaros.or.jp
[c] NEC Corporation, 1-10 Nisshin-cho, Fuchu-shi, Tokyo 183-0036 Japan, h-inada@bx.jp.nec.com

Commission VIII, ICWG IV/VIII

KEY WORDS: Onboard calibration, Sensitivity degradation, Fuel consumption, Contamination model, ASTER/VNIR

ABSTRACT:

Trend analysis of Terra/ASTER/VNIR calibration data is made for finding possible causes for degradation of radiometric calibration coefficients. Two sets of photometers are equipped at just after the onboard calibration lamp and at just in front of optics entrance of the mission instrument, VNIR. Unfortunately, the later was malfunctioned 300 days after the launch so that degradation of calibration optics which is situated in between calibration lamp and VNIR optics entrance is not monitored after that. The trends of calibration lamp response of VNIR within 300 days after the launch is very resemble to that of degradation of the later calibration lamp so that it might be possible to say that one of the possible causes of degradation VNIR response would be common. That might be a contamination at the optics entrance of VNIR which is later photo monitor is equipped due to plume impingement. From the spectral dependency, particle size of plume impingement is estimated. Also, it is confirmed that extrapolated trend is very similar to the onborad calibration data trend.

1. INTRODUCTION

Almost all the solar reflection channels of mission instruments onboard Earth observation satellite carry their own calibration system to maintain consistency of the radiometric fidelity of the instrument. Thus users may convert from the Digital Number, DN to radiance taking the onboard calibration system derived calibration coefficient into account. There are some reports on the calibration issues which include the Marine Observation Satellite-1 [Arai, 1988], Landsat-7 Enhanced Thematic Mapper Plus [Barker, et al., 1999], SeaWiFS [Barnes, et al., 1999], SPOT-1 and 2 [Gelleman, et al., 1993], Hyperion [Folkman, et al., 1997], and POLDER [Hagolle, et al., 1999]. Onboard calibrators cannot provide results of a higher accuracy than the preflight laboratory calibration. This means that the accuracy of the in-flight (absolute) calibration is inferior to the preflight results. This is because the preflight calibration source is used to calibrate the onboard calibrators. In addition, the uncertainty of the onboard calibrator typically increases with time. Hence, it makes good sense to include additional calibration approaches that are independent of the preflight calibration. Besides the normal and expected degradation of the onboard calibrators, they also run the risk of failing or operating improperly. Therefore, vicarious approaches are employed to provide further checks on the sensor's radiometric behavior.

As for the onboard calibration, given the understanding that the orbiting sensor's response will change over time, for instance, the ASTER: Airborne Sensor for Thermal Emission and Reflection calibration tem developed a methodology, based on OBC: Onboard Calibration results, to update pre-flight RCCs: Radiometric Calibration Coefficients that are input to generate the Level-1B (radiometrically and geometrically corrected DN) product [Thome, Arai et al., 2008]. Any electro-optical sensor is expected to degrade once in orbit, and therefore requires a mechanism to monitor the data's radiometric quality over time. Many sensors, including ASTER, employ onboard calibration devices to evaluate temporal changes in the sensor responses. Onboard calibrators in general, provide excellent temporal sampling of the sensor's radiometric behaviour over time. In addition, the repeatability and precision of the onboard systems allow use of these data in characterizing the sensor's response trends. Typical approaches for onboard calibration include lamp-based, diffuser-based, and detector-based methods. ASTER VNIR: Visible and Near Infrared Radiometer and SWIR: Short Wave Infrared Radiometer use lamp-based onboard calibrators. The specific design of the ASTER OBC is described in the following section. Then the sensor's response trends and suspected influence due to plume impingement of contamination of optics entrance of ASTER instrument is followed by with some evidences. Finally, discussions and concluding remarks are described.

2. CALIBERATION SYSTEM ONBOARD TERRA/ASTER/VNIR

2.1 Onboard calibration

ASTER VNIR and SWIR channels use lamp-based onboard calibrators for monitoring temporal changes in the sensor responses. Space restrictions aboard the Terra platform disallow a solar-based calibration, and therefore, onboard calibration is lamp-based. The VNIR and SWIR have two onboard calibration lamps, lamp-A and lamp-B. Both are used

periodically, and as a backup system. The VNIR calibration lamp output is monitored by a silicon photo monitor, and is guided to the calibration optics. The calibration optics output is itself monitored by a similar photo monitor that illuminates a portion of the VNIR aperture's observation optics. Meanwhile, the SWIR calibration assembly does not have a second silicon photo monitor. In the pre-flight phase, the onboard calibrators were well characterized with integration spheres calibrated with fixed freezing point blackbodies of Zn (419.5K), Pb (327.5K) and Sn (231.9K). This was accomplished by comparing the VNIR and SWIR output derived from the integration sphere's illumination of the two sensors. The same comparison was made by the calibration lamp's (A and B) illumination of the two sensors. Next, the pre-flight gain and offset data (no illumination) were determined. In addition, MTF: Modulation Transfer Function was measured with slit light from a collimator while stray light effect was measured with the integration sphere illumination, which is blocked at the full aperture of the VNIR and SWIR observation optics entrance. The pre-flight calibration data also includes (1) the spectral response, (2) out-of-band response, and (3) signal-to-noise ratio measured with a double grating monochromator.

The VNIR has two onboard calibration halogen lamps (A and B) as is shown in Fig.1.
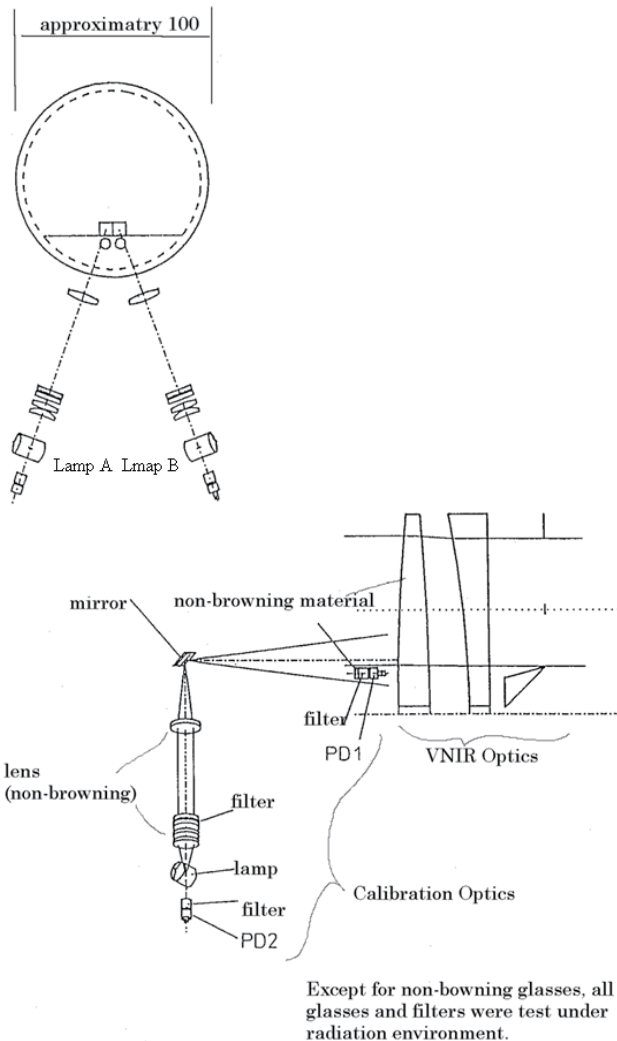

Fig.1 Onboard calibration system of the ASTER/VNIR

The light from these lamps is led to the VNIR optics via a set of calibration optics. Filters and photo-monitors are located fore

and aft of the calibration optics to monitor the output of the lamps as well as any possible degradation in the calibration optics. Lamp output and photo monitor data are collected every 33 days (primarily it was 16 days of the Terra orbital revisit cycle plus one day = 17 days), and RCC are calculated from the VNIR output taking into account the photo-monitor output. The RCC values are normalized by the pre-flight data to determine their final estimate. This procedure is the same for the SWIR RCC calculation except that the SWIR OBC does not include a photo monitor system at the lamp. Thus, only data from a photo monitor that is aft of the calibration optics are taken into account. The sources of VNIR and SWIR radiometric calibration uncertainties are shown in Table 1.

Table 1 Uncertainty in the absolute responsivity for normal gain mode of VNIR and SWIR at post launch phase
Uncertainty depends on the band (RSS of each band is 2.8, 3.9, 3.4, 5.2, 4.4, 3.9 for bands 4 to 9, respectively)

Source of uncertainty	VNIR Uncertainty (%)	SWIR Uncertainty (%)
Photomonitors sensitivity change due to temperature change	1.5	0.7
Degradation of photo-monitors	1.0	2.0
Photo-monitor output measurements	0.4	0.5
Lamp radiance change due to gravity shift	2.0	0.5-0.6
Radiometer output measurements	0.4	1.4-4.5
Lamp radiance change due to temperature change	N/A	1.0-1.2
Others (non-uniform contamination)	2.0	0.2
Root Sum Square (RSS)	3.4	2.8-5.2

The uncertainty in the band-to-band response ratio is 2.3% with the root sum square among 2.0% of the in-orbit lamp's spectral radiance changes. It registers 0.4% of the radiometer output measurements, and 1.0% of the others. Uncertainty in the detector-to-detector response ratio is 0.8% with the root sum square among 0.6% of the integration sphere, 0.4% of the radiometer output measurements, and 0.4% of the others. The most significant uncertainty is contamination and lamp radiance changes due to a gravity shift followed by photo-monitor sensitivity variations due to temperature changes and degradation.

The largest uncertainty is the radiometer output measurement followed by the photo monitor degradation, and lamp radiance dynamics due to temperature changes. Due to filter and detector sensitivity changes in the short wave infrared region, the uncertainty of the radiometer's output measurements are not so good, and vary by band. SWIR's absence of an aft photo monitor disallows monitoring the lamp output degradation, and hence, uncertainty in that regard is greater than that of VNIR. For the same reason, the uncertainty of the lamp radiance dynamics due to temperature changes is added to the VNIR uncertainty source. The influence due to non-uniform contamination of SWIR is smaller than that of VNIR because the SWIR wavelength coverage is longer than that of VNIR (Similar particle size for the same contamination material is assumed).

From these proto-flight model test data, and analyses derived with the previous mission instrument data, VNIR OBC is reliable at the 2% (1 sigma value) level while SWIR is at a 4% level. Thus the following RCC determination method is adopted The ASTER radiometric calibration coefficients are generated via the OBC data. The first three months of ASTER operation corresponded to the sensor activation and evaluation (A&E) phase during which the OBC results alone were used to determine the RCC. The OBC data have since been further evaluated by a panel of radiometric scientists relative to the VC results. The panel determined a set of trend equations used until a subsequent calibration panel review. The panel also determined the weightings used in the merging of the OBC and VC results. The best estimates of the ASTER RCC are publicized quarterly through newsletters, an Internet server, and other means. The user may then modify results obtained using the Level-1B product according to how large the difference is between the OBC results and the OBC-merged-with-VC results. The first panel meeting was held late during the A&E period to determine the weights for OBC and VC as well as version 1.0 radiometric calibration coefficients.

ASTER's current approach to determine the RCC for level-1 processing is as follows:

(1). Check for consistency between the halogen lamp system A and B. (System A and B are turned on every 17 days),

(2). Check for inter-channel dependency to find out if all bands within a telescope display similar tendencies

(3). Calculate RCC if both (1) and (2) are satisfied

(4). Calculate calibration coefficients based on cross-calibration results if (1) and (2) are not satisfied

(5). Calculate calibration coefficients based on other vicarious calibration data sets if (1) and (2) are not satisfied, and no cross-calibration coefficients exist

Basically, RCC for level-1 processing is determined with the current RCC, if the deviation of the current RCC is within a range of the uncertainty, 2% for VNIR and 4% for SWIR in comparison to the previous RCC. If the RCC trend shows inconsistent behaviour, then cross calibration and vicarious calibration are taken into account [Arai, 1994].

2.2 Onboard calibration trend

Fig.2 shows the RCC trends for VNIR. The RCC were changed relatively rapidly in the early stage of the launch, and is changed gradually for the time being. These are approximated with an exponential function with a bias and a negative coefficient. If the trend is approximated with the function of RCC = B exp (-At) + C, then A, B, and C equal the following values:

VNIR Band-1: A = 0.00190, B = 0.360, C = 0.735
      Band-2: A = 0.00168, B = 0.282, C = 0.807
      Band-3: A = 0.00150, B = 0.216, C = 0.860

During 2500 days after the launch, VNIR OBC RCC were degraded about 10% for Band-3, 16% for Band-2 and 23 % for Band-1, respectively while SWIR OBC RCC were degraded approximately 2.0 to 3.5% depending on bands. These trends are very similar to the vicarious calibration derived RCC, and also look similar to the OBC RCC trend of the Optical Sensor onboard the JERS-1 satellite, a legacy precursor to the ASTER instrument.

Each of the VNIR bands is shown, as are the onboard calibrator results for these bands in a fashion similar to that shown in Fig.2. On the other hand, Fig.3 shows vicarious calibration trend. Although both onboard and vicarious calibration trends

are similar, there are small biases, 1% for Band 1, -4% for Band 2 and -2% for Band 3, respectively as is indicated in Fig.3.
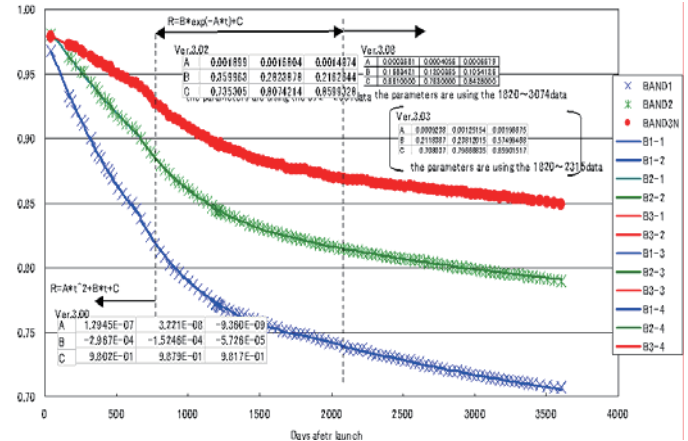

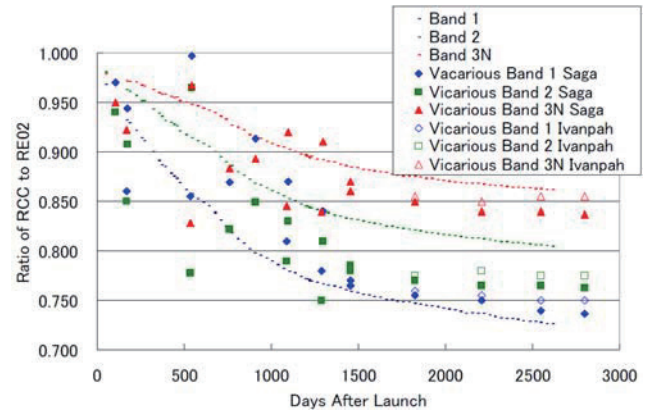Fig.2 OBC RCC trends for Band 1(Blue), Band 2(Green) and Band 3(Red)

Fig.3 OBC and vicarious RCC trends

Therefore, VNIR sensitivity degradation is confirmed with the different two sources. VNIR sensitivity degradation can be expressed with exponential function so that one of the possible causes of the degradation is contamination. The other causes are degradation of optical transparency of the calibration optics, sensitivity degradation of photo-monitor, degradation of photmonitor filter, etc.

2.3 Photo-monitor output trend

As is shown in Fig.1, VNIR has two photo-monitors, one (PD2) is set at lamp output and the other one (PD1) is set at the optics entrance, just in front of the collecting mirror.
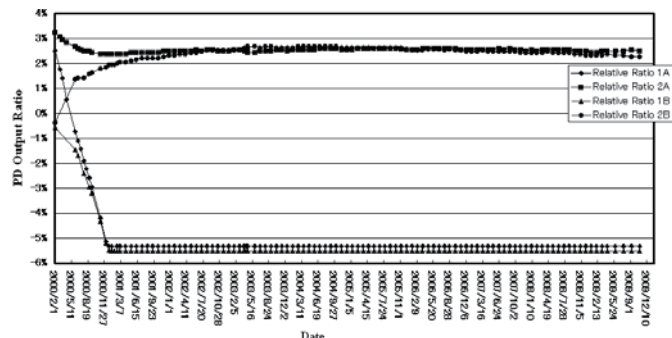

Fig.4 Photomonitor output for both calibration system A and B of PD1 and PD2.

Although PD1 output shows scale-off (under flow) at around 370 days after launch as is shown in Fig.4, the degradation of the degradation ratio shows almost same trend as OBC and vicarious RCC trends.

Also PD2 output shows stable lamp illumination so that one of possible causes for the sensitivity degradation is contamination at the optics entrance because the calibration optics is composed with browning lenses (less degradation of transparency due to radiation from solar flare).

From the PD1 output data, approximated exponential function is estimated with least square method. The degradation rate is confirmed to be almost same as OBC and vicarious RCC trends as is shown in Fig.5.
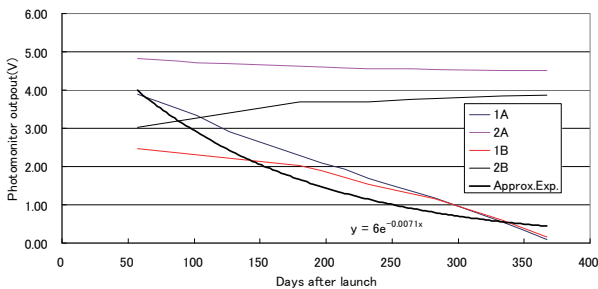
Fig.5 Approximated exponential function of PD1 output together with the other photomonitor output trends.

OBC RCC trends with reference to the calibration systems (Lamp A and B as well as photo-monitor PD1 and 2) are shown in Fig.6. The first three lines are for Band 3, 2 and 1, respectively, of RCC ranges from 105 (just after the launch) to 76 at around 3600 days after launch while the last four lines are for photo-monitor output. As is mentioned before, photo-monitor PD1 for both lamp A and B were in scale off at 370 days after launch so that PD1 (lamp A and B) trend were extrapolated by the exponential function with coefficients determined from the PD1 output data of the first 370 days. As is shown in Fig.6, the coefficients of exponential function of RCC trend is almost same as that of extrapolated function of PD1. Thus it might be concluded that one of the possible causes of the RCC degradation would be contamination at the optics entrance of VNIR due to plume impingement.
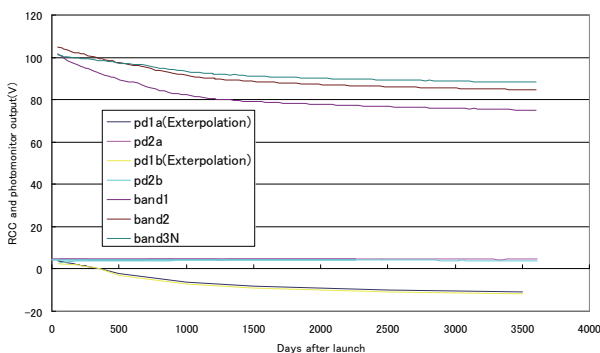

Fig.6 OBC RCC trend together with photo-monitor output trend.

From the wavelength dependency of OBC RCC trend, it is possible to estimate size distribution if it is assumed that plume impingement is one of possible causes of the RCC degradation. Fig.7 shows wavelength dependency of the RCC degradations. From this spectral dependency, size distribution is estimated

with the assumption that the size distribution is followed by the power law as well as the accumulated number of particles is normalized by one. Fig.8 shows the estimated size distribution. The size distribution estimation has not been validated yet.
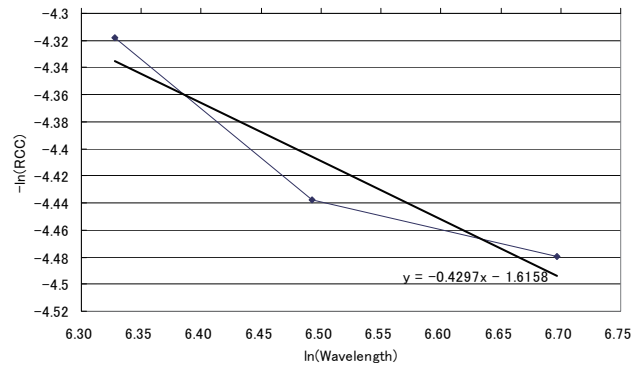

Fig.7 Spectral characteristics of RCC and its linearly approximated function.
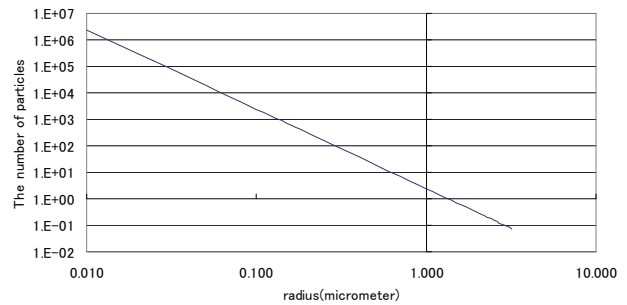

Fig.8 Estimated size distribution of plume impingement that is one of causes of the RCC degradation

2.4 Fuel consumption and RCC trend

Another evidence of the causes of RCC degradation is the relation between fuel consumption and RCC degradation. Fig.9 shows the fuel consumption of Terra satellite which carries ASTER/VNIR. Fig.9 also shows approximated function of the fuel consumption together with approximated function of RCC degradation. As is well known that the fuel consumption in just after launch is relatively large, there is bias between the two approximated functions of fuel consumption and RCC degradation. Both functions, however, show almost same trend.
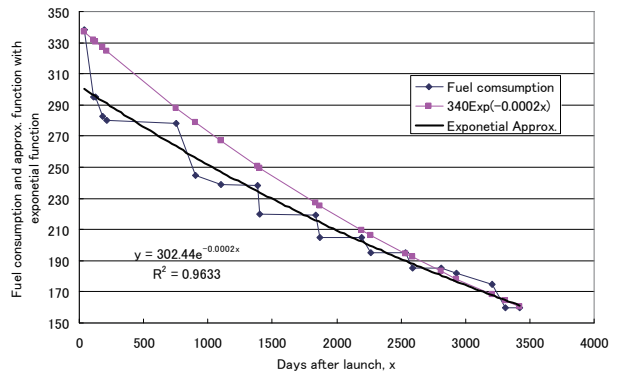

Fig.9 The relation between fuel consumption and RCC degradation.

Fig.10 also shows the OBC RCC trends, with the reference to the two calibration systems, Lamp A and B as well as PD2, for Band 1, 2 and 3. Fig.10 also shows the fuel consumption and its approximated function with exponential function. It may say that theses show almost same trend.
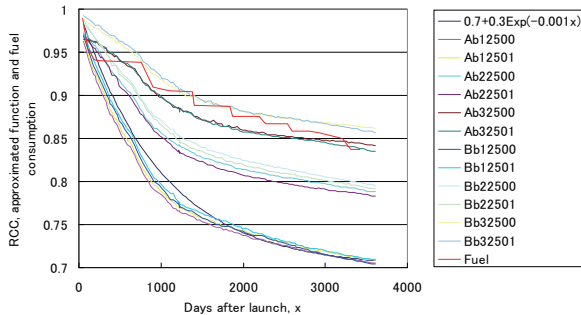

Fig.10 Relations between OBC RCC trend and fuel consumption as well as the approximated function of fuel consumption.
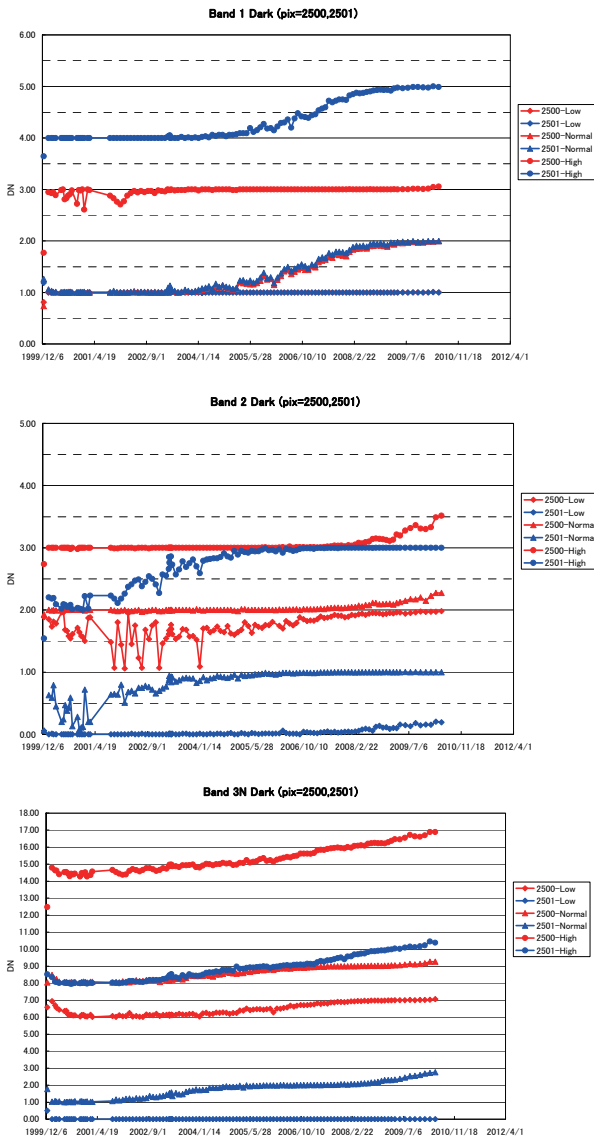

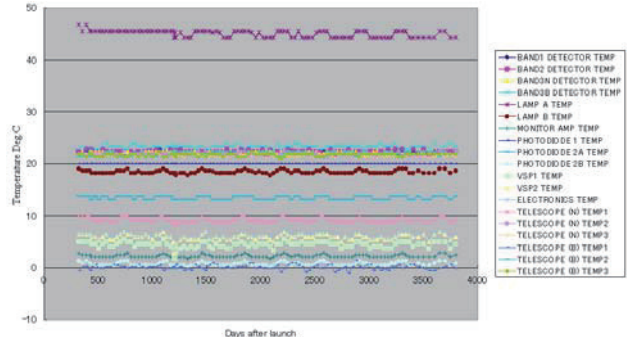Fig.11 Dark signals for Bands 1(Top),2(Middle),3(Bottom)

Fig.12 Detector temperature for Bands 1,2,3.

As is shown in Fig.11 and 12, dark signal (Output signal when no input from the VNIR optics entrance (Night time observation)) and detector temperature is very stable so that it may say that detector sensitivity is stable enough. Consequently, optics transparency would be a most suspected cause of the RCC (sensitivity) degradation due to plume impingement by hydrogen from the thrusters of Terra satellite because the RCC trend shows very resemble trend of fuel consumption.

3.CONCLUDING REMARKS AND DISCUSSIONS

It may concluded the followings,
(1) Similar trend is observed between OBC/RCC and photomonitor1 output when the photomonitor1 output trend is extrapolated for 3600 days, original trend is terminated with a 360 days though
(2) Assumption of which RCC degradation is caused by contamination of optics entrance of VNIR due to plume impingement from gas jet for attitude control seems to be correct
(3) Using wavelength dependency of RCC degradation, size distribution is estimated with the relation between ln(wavelength) and ln(RCC degradation) based on power low distribution function. It has to be validated though.

Consequently, optics transparency would be a most suspected cause of the RCC (sensitivity) degradation due to plume impingement by hydrogen from the thrusters of Terra satellite because the RCC trend shows very resemble trend of fuel consumption.

References

Arai K., Preliminary assessment of radiometric accuracy for MOS-1 sensors, International Journal of Remote Sensing, 9, 1, 5-12, 1988.

Arai, K., In-flight test site cross calibration between mission instruments onboard same platform, Advances in Space Research, 19, 9, 1317-1328, 1997.

Barker, J.L., S.K. Dolan, et al., Landsat-7 mission and early results, SPIE, 3870, 299-311, 1999.

Barnes, R.A., E.E.Eplee, et al., Changes in the radiometric sensitivity of SeaWiFS determined from lunar and solar based measurements, Applied Optics, 38, 4649-4664, 1999.

Gellman, D.I., S.F. Biggar, et al., Review of SPOT-1 and 2 calibrations at White Sands from launch to the present, Proc. SPIE, Conf.No.1938, 118-125, 1993.

Hagolle, O., P.Galoub, et al., Results of POLDER in-flight calibration, IEEE Trans. On Geoscience and Remote Sensing, 37, 1550-1566, 1999.

Herman B.M. and S. R. Browning, A numerical solution to the equation of radiative transfer, *J. Atmos. Sci.*, **22**:559-566, 1965.

Moran M.S., R. D. Jackson, G. F. Hart, P. N. Slater, R. J. Bartell, S. F. Biggar, D. I. Gellman, and R. P. Santer, "Obtaining surface reflectance factors from atmospheric and view angle corrected SPOT-1 HRV data," *Rem. Sens. Env.*, vol. 32, pp. 203-214, 1990.

Moran M.S., M. S., R. D. Jackson, P. N. Slater, and P. M. Teillet, "Evaluation of simplified procedures for retrieval of land surface reflectance factors from satellite sensor output," *Remote Sens. Environ.*, vol. 41, pp. 169-184, 1992.

Ono.A., F.Sakuma, K.Arai, et al., Pre-flight and Inflight Calibration for ASTER, Journal of Atmospheric and Ocean Technology, Vol.13, No.2, pp.321-335, Apr.,1996.

Slater P., K.Thome, A.Ono, F.Sakuma, K.Arai, et al., Radiometric Calibration of ASTER, Journal of Remote Sensing Society of Japan, Vol.15, No.2, pp.16-23, June 1995.

Thome, K., K. Arai, S.Tsuchida, S.Biggar, ASTER preflight and in-flight calibration and validation of level 2 products, IEEE Trans. on Geoscience and Remote Sensing, 36, 4, 1999.